Progress In Electromagnetics Research C, Vol. 106, 229–238, 2020

A Novel Small Size CPW-Fed Slot Antenna with Circular Polarization for 5G Application

Seyyedeh F. Seyyedrezaei[1], Hamid R. Hassani[1], Maryam Farahani[2], and Sajad Mohammad-Ali-Nezhad[2, *]

Abstract—A novel CPW-fed circular polarized slot printed monopole antenna for 5G application is presented. The proposed slot monopole antenna occupies a small area of $0.23\lambda_o \times 0.35\lambda_o \times 0.019\lambda_o$, and the wavelength has been obtained for the center frequency of 3.4 GHz to 3.8 GHz range. First, two square slots are inserted on either side of the feed line, and to provide two orthogonal electric fields, a spiral stub is embedded in one of the slots. In order to improve the axial ratio bandwidth of the proposed antenna, it is possible to etch another spiral stub on the other side of the feed line. The proposed antenna provides circular polarized radiation such that the reflection coefficient bandwidth (below −10 dB) is about 1.4 GHz (from 2.9 GHz to 4.3 GHz) or 38.89%, and the axial ratio bandwidth below 3 dB is about 400 MHz, from 3.4 GHz to 3.8 GHz. This is 11.1% at center frequency of 3.6 GHz. This antenna covers the useful frequency bandwidth for 5G application. Simulation and measurement results are presented.

1. INTRODUCTION

Regarding the rapid development and growth of wireless communication and 5G (5th generation mobile network), it is essential to satisfy the increasing network requests. It is expected that 5G would propose significantly higher throughput than the LTE (long-term evolution), and it is able to activate new business models, applications, and industries and enhance the life quality throughout the world through exceptional use cases which need communications with high data-rate, low latency, and massive connectivity for applications such as autonomous vehicles, smart cities, smart homes, mobile, and Internet of Things (IoT) [1, 2].

One of the factors which affects the realization of 5G communication significantly is antenna design. Hence, wide bandwidth, simple structure antennas have attracted attention [3–7]. In [5], a 5G wideband patch antenna fed by an L-shaped probe has been presented. The authors of [6] have presented a parasitic layer-based radiation pattern reconfigurable dipole antenna capable of 3-D beamsteering. The authors of [7] have presented parallel metal via holes which can be used instead of the quarter-wavelength shorted patch for a Magneto-Electric-dipole.

Compared to linear polarization (LP), channel performance and mobility and orientation freedom of circular polarization (CP) radiation pattern are better, and its multipath interference and fading are lower. A few studies on 5G technology have investigated the operation of CP antennas. These antennas mainly operate in the mm-wave band [8, 9].

It seems that the best candidate is Printed CPW-fed slot monopole antenna due to its low profile, low radiation loss, wide impedance bandwidth, no soldering points for printing on the circuit board of the portable devices, and easy fabrication with low cost [10–27].

Received 7 August 2020, Accepted 29 October 2020, Scheduled 9 November 2020

* Corresponding author: Sajad Mohammad-Ali-Nezhad (s.mohammadalinezhad@qom.ac.ir).

[1] Electrical & Electronic Engineering Department, Shahed University, Tehran, Iran. [2] Electrical & Electronic Engineering Department, University of Qom, Qom, Iran.

In [11], the authors presented a C-shaped microstrip asymmetrical antenna for achieving circular polarization. This antenna uses an aperture coupling at the center for feeding, which enables CP operation. This antenna has a 3 dB AR bandwidth about 3.3%, and its overall size is $0.48\lambda_o \times 0.48\lambda_o \times 0.092\lambda_o$ at 2.4 GHz. In [12], a circularly polarized microstrip annular slot antenna with a total size of $0.58\lambda_o \times 0.77\lambda_o$ at the frequency of 2.9 GHz was proposed. The authors of [15] have presented a dual-band and sense circularly polarized CPW-fed monopole antenna whose two parasitic elements are rectangular, and it has an I-shaped stub. In [16], a reconfigurable slot antenna for circular polarization has been reported. With this antenna, the 3 dB AR bandwidth is around 1%, and the overall antenna size is $0.67\lambda_o \times 0.67\lambda_o \times 0.02\lambda_o$ at 1.5 GHz. A Broadband CPW-Fed Circularly-Polarized Antenna With an Open Slot has been presented in [18], and the overall antenna size is $0.61\lambda_o \times 0.61\lambda_o$ at 3.7 GHz. In [24], a CPW-fed square slot antenna with the overall size of $0.4\lambda_o \times 0.4\lambda_o$ at 2.5 GHz for circular polarization characteristics, with the 3 dB AR bandwidth of 12%, has been proposed.

Table 1 compares the proposed CPW-fed or slot antenna with other CP antennas. The proposed antenna is better than others, concerning the antenna size.

Table 1. Comparison between the proposed design and others.

Slot Antenna	**CPW -Fed**	**Gain (dBi)**	**Impedance bandwidth**	**Axial ratio bandwidth (GHz)**	**f (GHz)**	**Antenna Size (λ)**	**Ref.**
*	*		2.2–2.6	2.35–2.45	2.4	$0.24 * 0.32 * 0.019$	[10]
*			5–6	5.15–5.75	5.4	$0.54 * 0.54 * 0.018$	[12]
	*	1.5–2.5	1.81–3.83	2.2–2.9	2.5	$0.52 * 0.62 * 0.01$	[15]
*		2.55	1.45–1.55	1.52–1.535	1.5	$0.67 * 0.67 * 0.02$	[16]
*		2–3	3.25–3.55	3–3.6	3.4	$0.38 * 0.38 * 0.03$	[17]
*	*	3.7 (at 2.4 GHz)	2.3–3.9	2.3–3.15	2.65	$0.35 * 0.53 * 0.01$	[19]
*	*	3–4	1.78–5.64	2.85–5.21	4	$0.66 * 0.66 * 0.013$	[20]
*	*	2.5–3.4	1.73–3.11	1.98–2.95	2.5	$0.83 * 1 * 0.007$	[21]
*	*	3–4	2.2–3.2	2.2–3.2	2.7	$0.33 * 0.5 * 0.007$	[22]
*	*		2.19–3.07	2.23–2.65	2.45	$0.4 * 0.4 * 0.013$	[23]
*	*	3–4	172–294	2.06–2.76	2.4	$0.5 * 0.5 * 0.006$	[24]
*	*	2.9–3.3	1.69–2.78	2.26–2.47	2.35	$0.4 * 0.47 * 0.007$	[25]
*	*	2.3–3.8	2.16–3.9	2.06–2.71	2.38	$0.42 * 0.42 * 0.008$	[26]
*	*	2–3.8	2.6–2.8	2.3–2.5	2.4	$0.4 * 0.4 * 0.013$	[27]
*	*	3.2–4	2.9–4.3	3.4–3.8	3.6	$0.23 * 0.35 * 0.019$	Proposed Antenna

In most of the studies mentioned above, the antennas are not compact and not suitable for 5G. In this paper, a new circularly polarized CPW-fed slot antenna is presented for the use in 5G applications. In the ground plane, two similar slots are placed on both sides of the feed line. In each of the slots a spiral stub is etched leading to circularly polarized radiation. The proposed antenna occupies a small area of $0.23\lambda_o \times 0.35\lambda_o \times 0.019\lambda_o$, and the axial ratio bandwidth is about 400 MHz (3.4 to 3.8 GHz) or about 11% with respect to the centre frequency at 3.6 GHz.

2. ANTENNA DESIGN

In this section, the antenna design procedure will be explained. This section consists of two parts. In part (a), the initial antenna structure will be presented, and in part (b) the improved structure will be explained.

Two equal amplitude orthogonal fields with quadrature phase difference are required for achieving circularly polarized radiation.

2.1. Single Spiral Stub Antenna Structure

Figure 1 shows the initial CPW-fed antenna structure, which is similar to a spiral antenna, to produce the circular polarization. In this structure, two square slots are inserted on both sides of the feed to provide two orthogonal electric fields, and a spiral stub is embedded in one of the slots. This CPW-fed defected ground structure (DGS), with the single spiral slot, radiates a circularly polarized field. As can be seen from Fig. 1, to provide a better impedance matching and consequently better impedance bandwidth, the width of the feed is reduced, and a gap is introduced along its length. The presence of the square slot in the right hand side of the structure in Fig. 1 does not contribute to radiation, but it affects the resonance frequency of the structure.

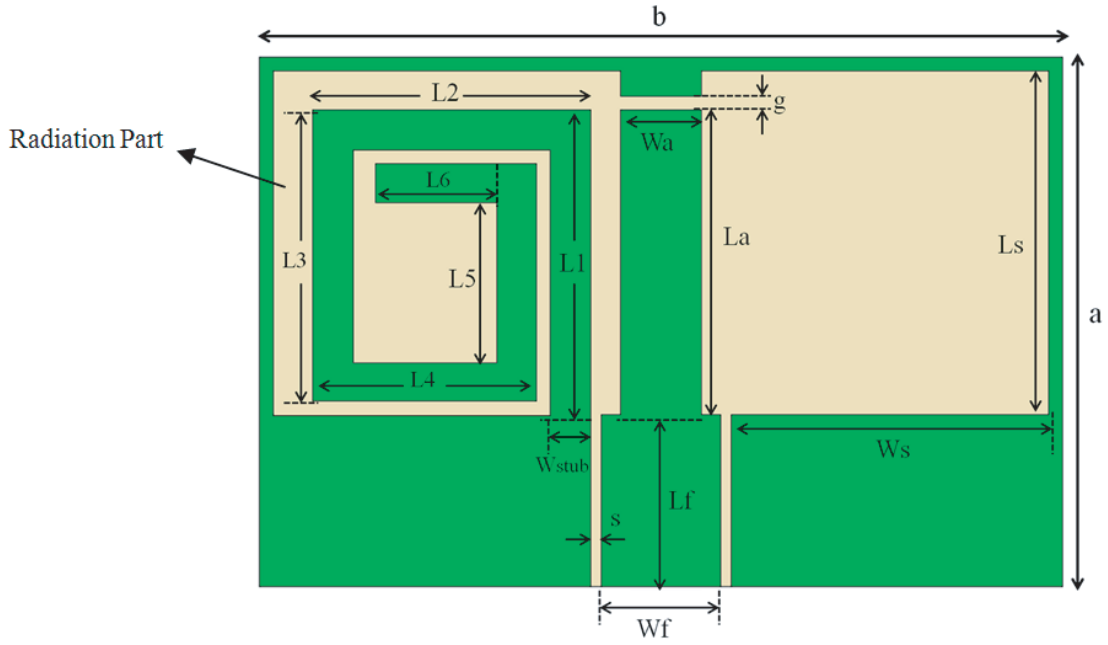

Figure 1. The proposed single spiral stub antenna.

In this structure, an FR4 substrate with $\varepsilon_r = 4.4$ and a thickness of 1.6 mm is utilized. The total size of this configuration equals $20 \times 30\,\text{mm}^2$; the remaining dimensions of the proposed antenna are presented in Table 2.

To give an explanation of CP radiation mechanism, the current distribution of this antenna at the resonance frequency of 3.6 GHz at different time intervals is shown in Fig. 2. The magnetic current distribution or the tangential electric field vector in the slots must be evaluated and explored since the radiation originates from the spiral slots. It is observed at $\omega t = 0$ degrees; the total electric field vector has a direction as shown in Fig. 2. In $\omega t = 90$ degrees, the direction of the total electric field vector rotates by 90 degrees with respect to 0 degree total vector. Similarly, at $\omega t = 180$ and 270 degrees, the total electric field vector has a rotation of 90 degrees in each step as illustrated in Fig. 2.

According to Fig. 2, the direction of the total electric field vector follows a clockwise path from $\omega t = 0$ to $\omega t = 270$ degrees, when one looks at the antenna from its top surface. Therefore, it results in LHCP radiation along the normal direction to the antenna. On the contrary, looking at the antenna

Table 2. Dimensions of the initial and improved proposed antennas.

Dimension (mm)	a	b	Lf	Wf	s	Wa	La	g	Ls
Initial antenna	20	30	6.5	4.5	0.4	3	11.3	0.5	14
Improved antenna	20	30	6.5	4.5	0.4	3	10.8	0.5	14
Dimension (mm)	a	b	Lf	Wf	s	Wa	La	g	Ls
Initial antenna	11.58	1.5	12.5	11	11.5	9	6.5	4.5	-
Improved antenna	10.85	1.5	11.8	10.35	10.5	8.35	5.5	4.85	3.5

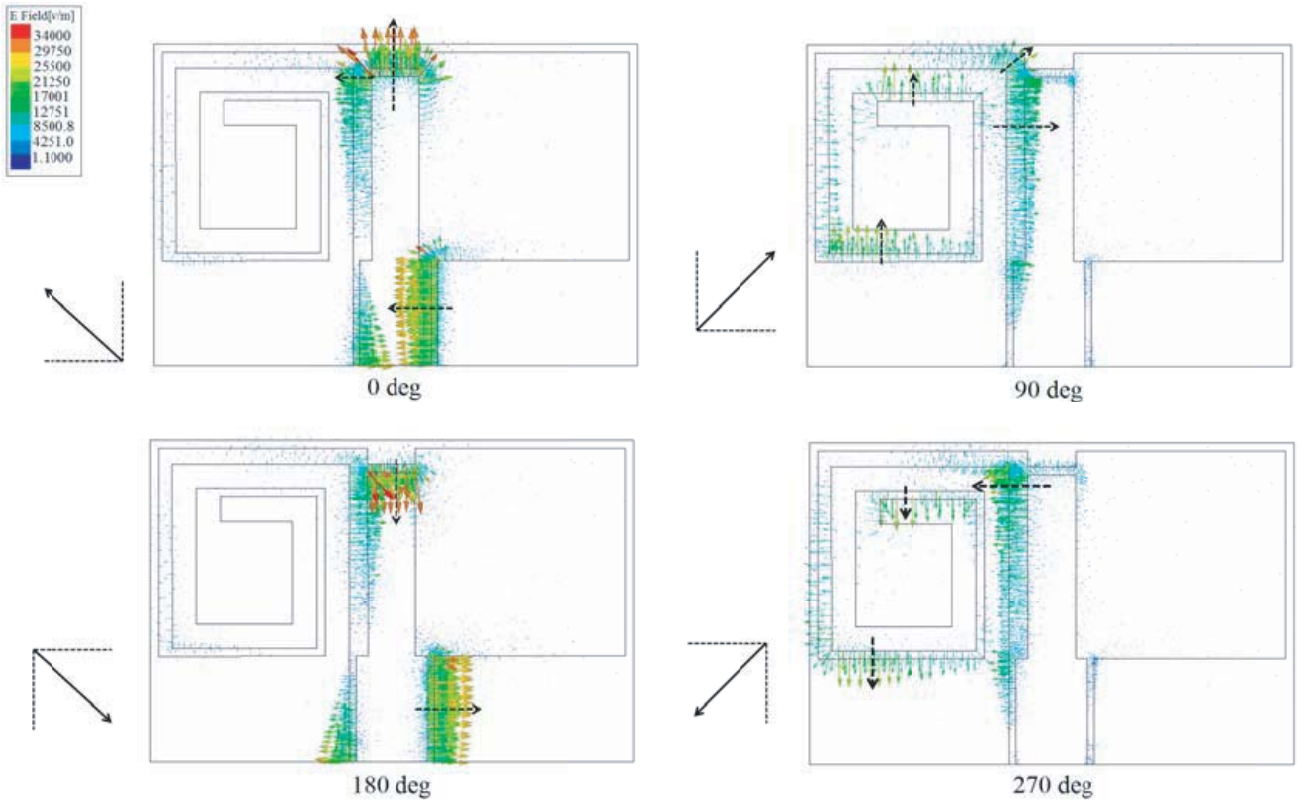

Figure 2. The simulated electric field vector for the proposed single spiral stub antenna at the frequency of 3.6 GHz for different input signal phases.

from the bottom surface shows a counter clockwise rotation which depicts RHCP. It is worth mentioning that different frequencies in the operational band exhibit the same behaviour.

2.2. Double Spiral Stub Antenna with Improved Bandwidth

By etching another spiral stub on the other side of the feed, it will be shown that the axial ratio of the slot antenna improves, and a better circularly polarized structure will be achieved. This improved double spiral stub structure is shown in Fig. 3. Much like the structure presented previously, here we also utilize an FR4 substrate with a thickness of 1.66 mm and $\varepsilon_r = 4.4$. The total size for this configuration equals $20 \times 30\,\text{mm}^2$, while the remaining dimensions are presented in Table 2.

Similar to the previous section, to study the CP radiation mechanism, the magnetic current distribution or equivalently tangential electric field vector on this antenna at the resonance frequency

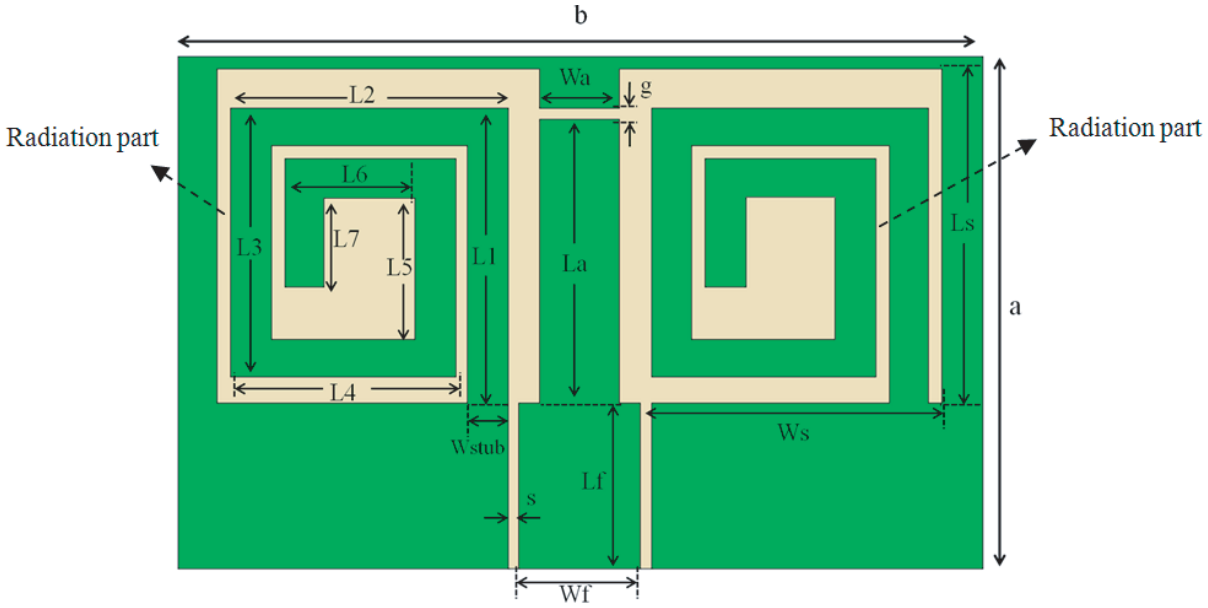

Figure 3. The improved antenna structure.

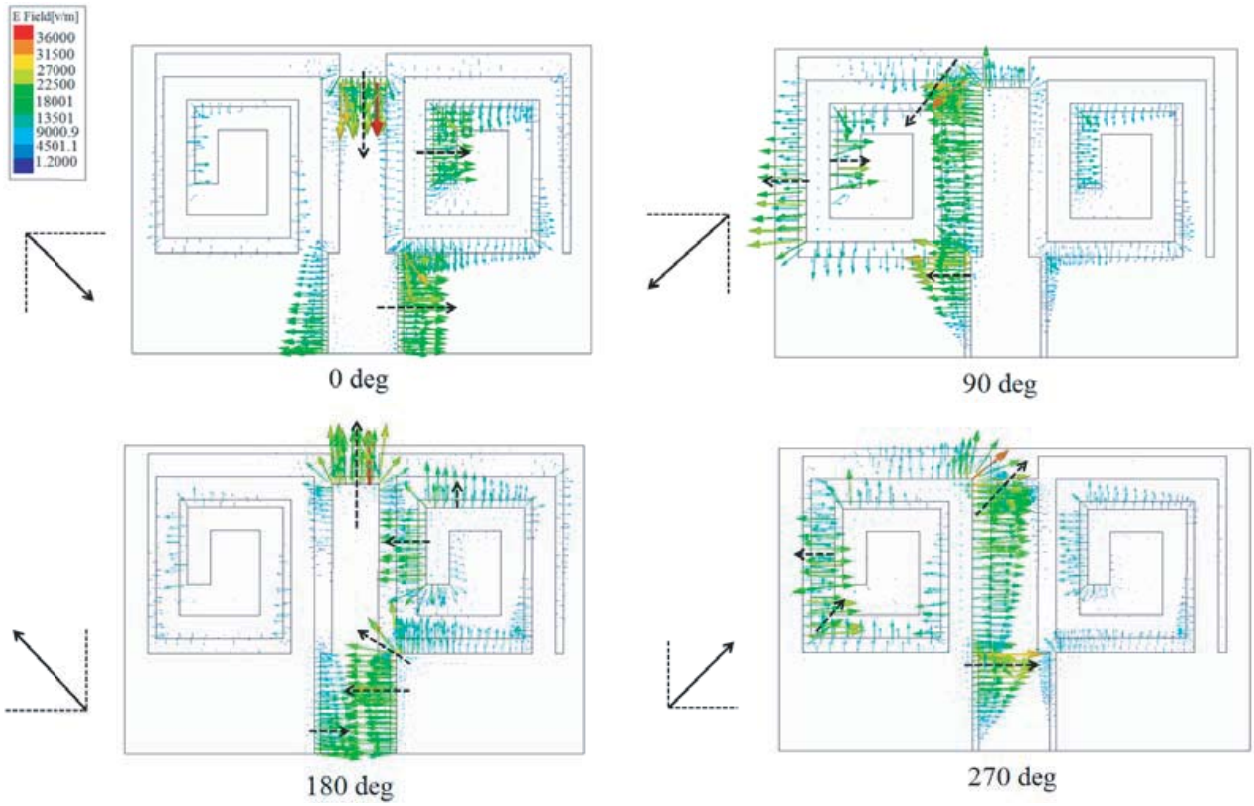

Figure 4. Simulated electric field vector on the improved double spiral stub antenna at 3.6 GHz.

of 3.6 GHz at different time intervals is shown in Fig. 4. It can be seen that at $\omega t = 0$ degrees the total tangential electric field vector has a direction as shown in Fig. 4. At $\omega t = 90$ degrees, the direction of the total tangential electric field vector rotates by 90 degrees. Similarly, at $\omega t = 180$ and 270 degrees the total current distribution vector rotates 90 degrees further in each step as shown in Fig. 4.

According to Fig. 4, the direction of the total electric field vector follows a clockwise path from $\omega t = 0$ to $\omega t = 270$ degrees, when one look at the antenna from its top surface. Therefore, it results in LHCP radiation along the normal direction to the above antenna. By interchanging the position of the left spiral stub and right spiral, the LHCP radiation can be changed to RHCP radiation. It is worth mentioning that different frequencies in the operational band exhibit the same behaviour.

3. SIMULATION AND MEASUREMENT RESULTS

The single spiral stub antenna structure and the improved version, the double spiral stub antenna, are simulated through the Ansoft HFSS software package, and both antennas are also fabricated. The fabricated antennas are shown in Fig. 5. Antenna characteristics including axial ration, reflection coefficient, and radiation patterns are discussed in this section.

The reflection coefficient for the presented single spiral stub antenna is depicted in Fig. 6. Based on this figure, it can be concluded that with a reflection coefficient of -10 dB, the proposed antenna can enable a bandwidth of 1070 MHz (increased from 2.81 GHz), which is an increase about 31.99 percent, covering the frequency bands of 5G applications.

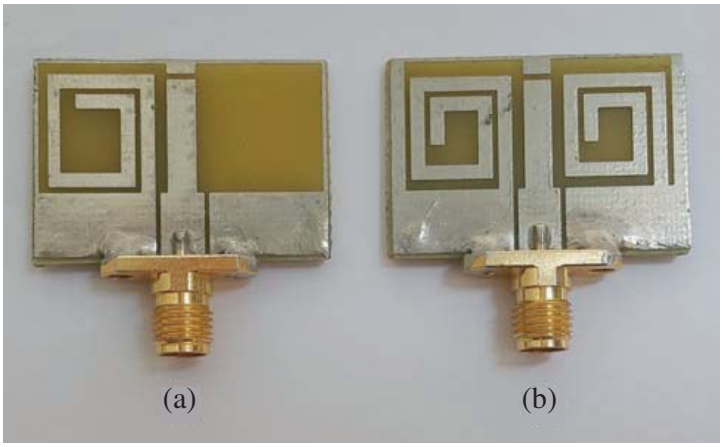

Figure 5. The fabricated antennas. (a) Single spiral stub and (b) double spiral stub.

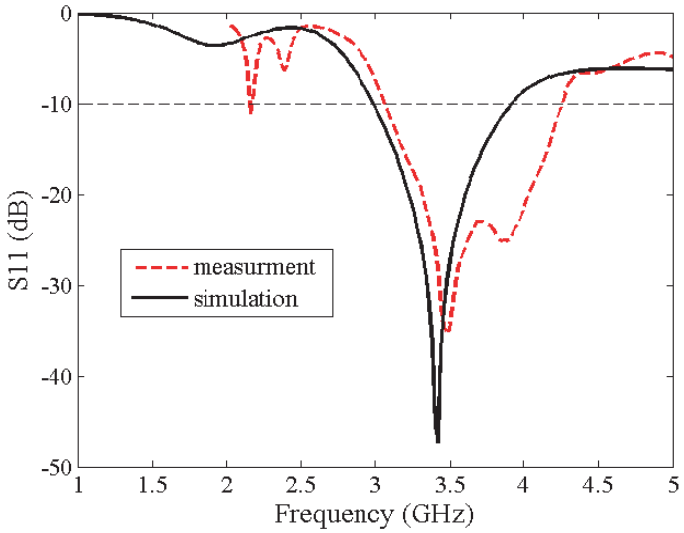

Figure 6. Reflection coefficient of the proposed single spiral stub antenna.

The proposed double spiral stub antenna improves the reflection coefficient bandwidth, reaching a value of 1.4 GHz (increased from 2.9 GHz), which is about 38.89 percent compared to the central frequency of 3.6 GHz. This can also be seen in Fig. 7. Based on the simulation and measurement results depicted in Fig. 7, the two are in good agreement.

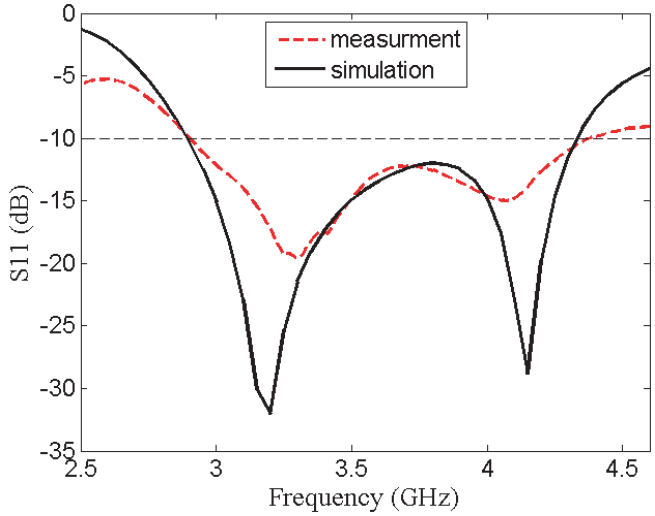

Figure 7. Reflection coefficient of the improved double spiral stub antenna.

The axial ratio response of the proposed antenna at the broadside direction is shown in Fig. 8. This antenna reaches a 3 dB radio bandwidth of 200 MHz.

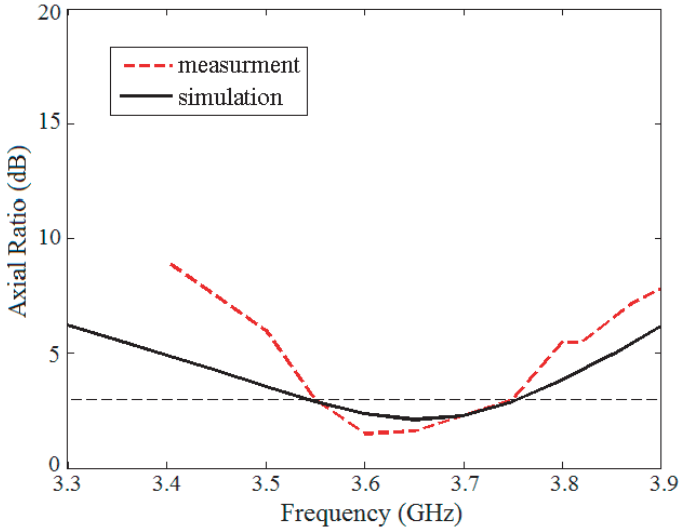

Figure 8. Axial Ratio of the single spiral stub antenna.

Figure 9 represents the axial ratio response of the enhanced double spiral stub antenna which has a 3 dB axial ratio bandwidth about 400 MHz (3.4 to 3.8 GHz) which is about 11% regarding the center frequency at 3.6 GHz. Considering the above results, it can be said that the double spiral stub antenna structure outperforms the single spiral stub structure in terms of CP operation bandwidth.

This increase in impedance bandwidth and axial ratio is due to the existence of two spiral paths with different dimensions. This increase in bandwidth would not have occurred if the first spiral path

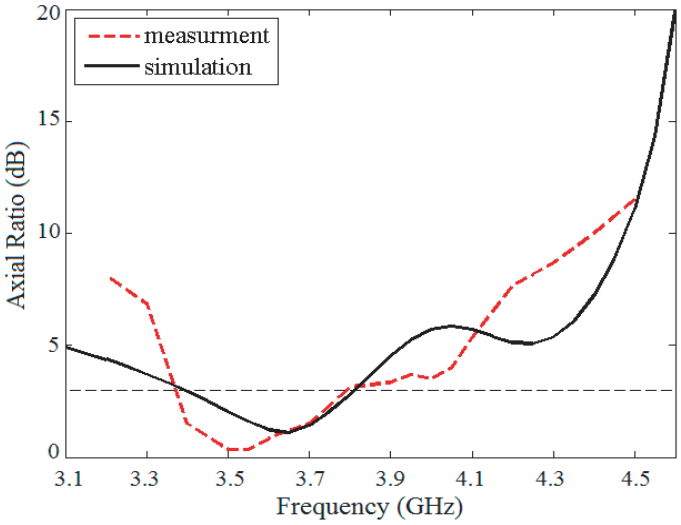

Figure 9. Axial Ratio of the improved structure.

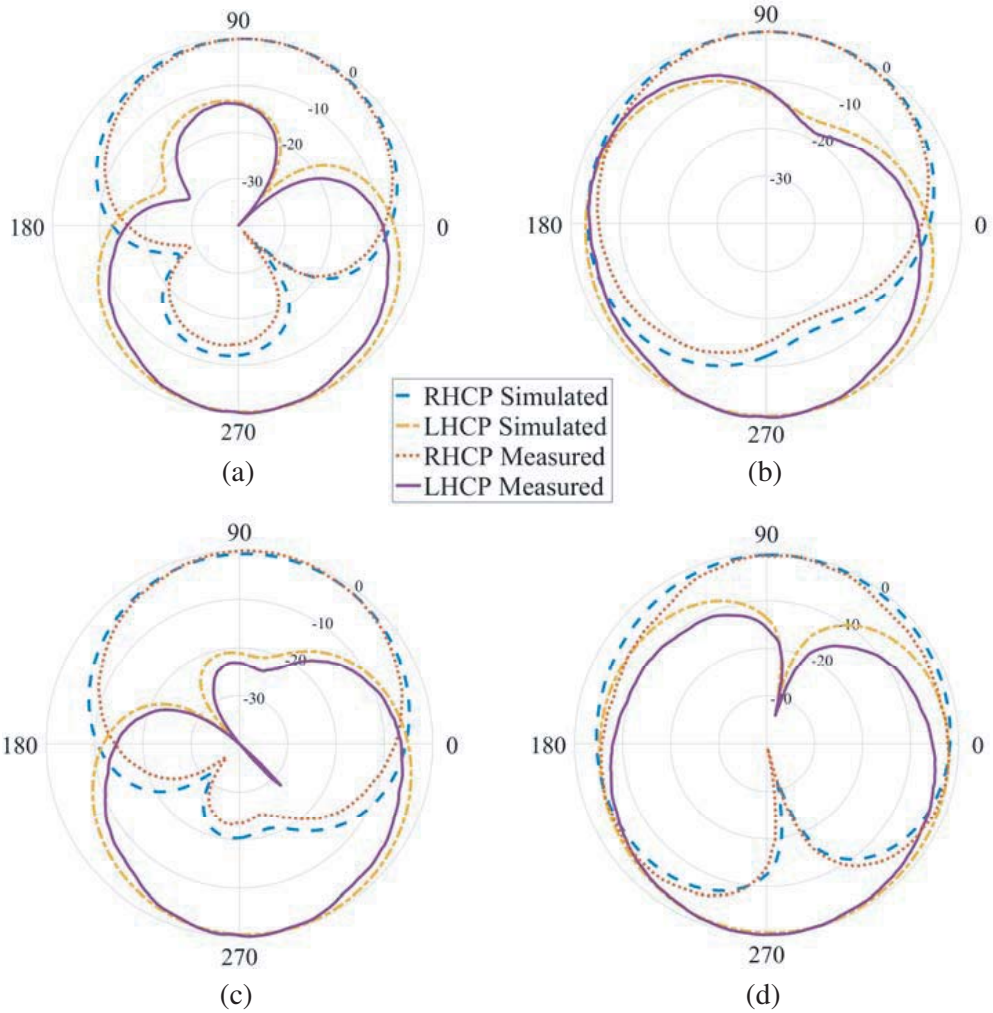

Figure 10. Measured and simulated RHCP and LHCP radiation patterns for the proposed antenna at a frequency of 3.6 GHz. (a) E-plane and (b) H-plane patterns for the proposed antenna; (c) E-plane and (d) H-plane radiation patterns of the double spiral stub antenna.

were exactly symmetrical to the feed line. However, the second slot path is smaller than the first path, and this causes two paths with different lengths to be created. In other words, two resonant paths were created, and circular polarization was created in two frequency ranges.

Simulation and measurement of LHCP and RHCP radiation patterns of the single and double spiral stub antennas at the center frequency of 3.6 GHz are shown in Fig. 10. It can be seen that cross-polarization of the single spiral stub antenna at the boresight direction is about 14 dB lower than the co-polarization with the 3 dB AR beamwidths of about 105 degrees. cross-polarization of the double spiral stub antenna at the bore sight direction is about 24 dB lower than the co-polarization with the 3 dB AR beamwidths of about 120 degrees.

4. CONCLUSION

a new circularly polarized CPW-fed slot antenna is presented for the use in 5G applications. The size of the antenna is $20 \times 30\,\text{mm}^2$, and it can be mounted on an affordable FR4 substrate, which is 1.66 mm thick and has a relative permittivity of 4.4. First, two square slots are inserted on both sides of the feed, and a spiral stub is embedded in one of those slots. So, an antenna structure with a reflection coefficient bandwidth of 1070 MHz (from 2.81 to 3.88 GHz) or about 32% is achieved, which provides the 3 dB axial ratio bandwidth of 5.5% (from 3.55 to 3.75 GHz). Then, by etching another spiral stub on other side of the feed, the axial ratio bandwidth is improved, so that the axial ratio bandwidth is about 400 MHz (from 3.4 to 3.8 GHz) or about 11% with respect to the center frequency at 3.6 GHz, with the reflection coefficient bandwidth about 1.4 GHz from 2.9 to 4.3 GHz (38.89%), which covers useful frequency bandwidth for 5G application. Therefore, the improved antenna structure demonstrates good improvement in CP operation bandwidth with respect to the initial structure. For both structures, the simulation result is compared with those obtained from the measurement, and good agreement is shown. To explain the CP radiation mechanism, the current distribution of these antennas at the resonance frequency of 3.6 at different time intervals has been studied.

REFERENCES

1. Gupta, A. and R. K. Jha, "A survey of 5G network: Architecture and emerging technologies," *IEEE Access*, Vol. 3, 1206–1232, 2015.
2. Arya, A. K., S. J. Kim, S. Park, D.-H. Kim, R. S. Hassan, K. Ko, and S. Kim, "Shark-fin antenna for railway communications in LTE-R, LTE, and lower 5G frequency bands," *Progress In Electromagnetics Research*, Vol. 167, 83–94, 2020.
3. Wei, G. and Q. Feng, "Dual-band MIMO antenna array for compact 5G smartphones," *Progress In Electromagnetics Research C*, Vol. 99, 157–165, 2020.
4. Khan, R., A. A. Al-Hadi, P. J. Soh, M. R. Kamarudin, M. T. Ali, and Owais, "User influence on mobile terminal antennas: A review of challenges and potential solution for 5G antennas," *IEEE Access*, Vol. 6, 77695–77715, 2018.
5. Parchin, N. O., H. J. Basherlou, and R. A. Abd-Alhameed, "Dual circularly polarized crescent-shaped slot antenna for 5G front-end systems," *Progress In Electromagnetics Research Letters*, Vol. 91, 41–48, 2020.
6. Hossain, M. A., I. Bahceci, and B. A. Cetiner, "Parasitic layer-based radiation pattern reconfigurable antenna for 5G communications," *IEEE Transactions on Antennas and Propagation*, Vol. 65, No. 12, 6444–6452, 2017.
7. Lai, H. W. and H. Wong, "Substrate integrated magneto-electric dipole antenna for 5G Wi-Fi," *IEEE Transactions on Antennas and Propagation*, Vol. 63, No. 2, 870–874, 2015.
8. Hussain, N., M. Jeong, J. Park, and N. Kim, "A broadband circularly polarized fabry-perot resonant antenna using a single-layered PRS for 5G MIMO applications," *IEEE Access*, Vol. 7, 42897–42907, 2019.
9. Wu, Q., J. Hirokawa, J. Yin, C. Yu, H. Wang, and W. Hong, "Millimeter-wave multibeam endfire dual-circularly polarized antenna array for 5G wireless applications," *IEEE Transactions on Antennas and Propagation*, Vol. 66, No. 9, 4930–4935, 2018.

10. Seyyedrezaei, S. F., H. R. Hassani, and S. Mohammad-Ali-Nezhad, "A novel small size CPW-fed circular polarized antenna," *Loughborough Antennas & Propagation Conference*, 1–4, Loughborough, 2011.
11. Elboushi, A., O. Haraz, and A. Sebak, "High gain circularly polarized slot coupled antenna for millimeter wave applications," *Microwave and Optical Tech. Lett.*, Vol. 56, No. 11, 2522–2526, 2014.
12. Beigmohammadi, G., Ch. Ghobadi, J. Nourinia, and M. Ojaroudi, "Small square slot antenna with circular polarisation characteristics for WLAN/WiMAx applications," *Electron. Lett.*, Vol. 46, 672–673, 2010.
13. Liu, Y., K. Huang, Y. Yang, and B. Zhang, "A low-profile lightweight circularly polarized rectenna array based on coplanar waveguide," *IEEE Antennas and Wireless Propagation Letters*, Vol. 17, 1659–1663, 2018.
14. Liu, H., Y. Liu, and S. Gong, "Broadband microstrip-CPW fed circularly polarised slot antenna with inverted configuration for L-band applications," *IET Microwave, Antennas & Propagation*, Vol. 11, 880–885, 2017.
15. Saini, R. K., S. Dwari, and M. K. Mandal, "CPw-fed dual-band dual-sense circularly polarized monopole antenna," *IEEE Antennas and Wirelless Propagation Letters*, Vol. 16, 2497–2500, 2017.
16. Nishamol, M. S., V. P. Sarin, D. Tony, C. K. Aanandan, P. Mohanan, and K. Vasudevan, "An electronically reconfigurable microstrip antenna with switchable slots for polarization diversity, *IEEE Transactions on Antennas and Propagation*, Vol. 59, 3424–3427, 2011.
17. Al-Yasir, Y. I. A., A. S. Abdullah, N. Ojaroudi Parchin, R. A. Abd-Alhameed, and J. M. Noras, "A new polarization-reconfigurable antenna for 5G applications," *Electronics*, Vol. 7, 293–301, 2018.
18. Jan, J., C. Pan, K. Chiu, and H. Chen, "Broadband CPW-fed circularly-polarized slot antenna with an open slot," *IEEE Transactions on Antennas and Propagation*, Vol. 61, 1418–1422, 2013.
19. Wang, C. and C. Chen, "CPW-fed stair-shaped slot antennas with circular polarization," *IEEE Transactions on Antennas and Propagation*, Vol. 57, 2483–2486, 2009.
20. Li, G., H. Zhai, T. Li, L. Li, and C. Liang, "CPW-fed S-shaped slot antenna for broadband circular polarization," *IEEE Antennas and Wireless Propagation Letters*, Vol. 12, 619–622, 2013.
21. Xue, H., X. Yang, and Z. Ma, 2015, "A novel microstrip-CPW fed planar slot antenna with broadband and circular polarization," *IEEE Antennas and Wireless Propagation Letters*, Vol. 14, 1392–1395.
22. Sze, J., C. G. Hsu, Z. Chen, and C. Chang, "Broadband CPW-fed circularly polarized square slot antenna with lightening-shaped feedline and inverted-L grounded strips," *IEEE Transactions on Antennas and Propagation*, Vol. 58: 973–977, 2010.
23. Chang, K.-M., R.-J. Lin, I.-C. Deng, J.-B. Chen, K. Q. Xiang, and C. J. Rong, "A novel design of a CPW-fed square slot antenna with broadband circular polarization," *Microw. Opt. Technol. Lett.*, Vol. 48, 2456–2459, 2006.
24. Sze, J. and C. Chang, "Circularly polarized square slot antenna with a pair of inverted-L grounded strips," *IEEE Antennas and Wireless Propagation Letters*, Vol. 7, 149–151, 2008.
25. Wang, C. and C. Lin, "A CPW-fed open-slot antenna for multiple wireless communication systems," *IEEE Antennas and Wireless Propagation Letters*, Vol. 11, 620–623, 2012.
26. Chen, L., X. Ren, Y.-Z. Yin, and Z. Wang, "Broadband CPW-fed circularly polarized antenna with an irregular slot for 2.45 GHz RFID reader," *Progress In Electromagnetics Research Letters*, Vol. 41, 77–86, 2013.
27. Sim, C.-Y., H.-D. Chen, L. Zuo, and T.-A. Chen, "CPW-fed square ring slot antenna with circular polarization radiation for WiMAX/WLAN applications," *Microw. Opt. Technol. Lett.*, Vol. 57, 886–891, 2015.